

Fluorescent ADP Sensing in Physiological Conditions Based on Cooperative Inhibition of a Miniature Esterase

Laurent Vial and Pascal Dumy*

Département de Chimie Moléculaire, UMR-5250, ICMG FR-2607, CNRS - Université Joseph Fourier, BP 53, 38041 Grenoble Cedex 9, France

Received February 1, 2007; E-mail: pascal.dumy@ujf-grenoble.fr

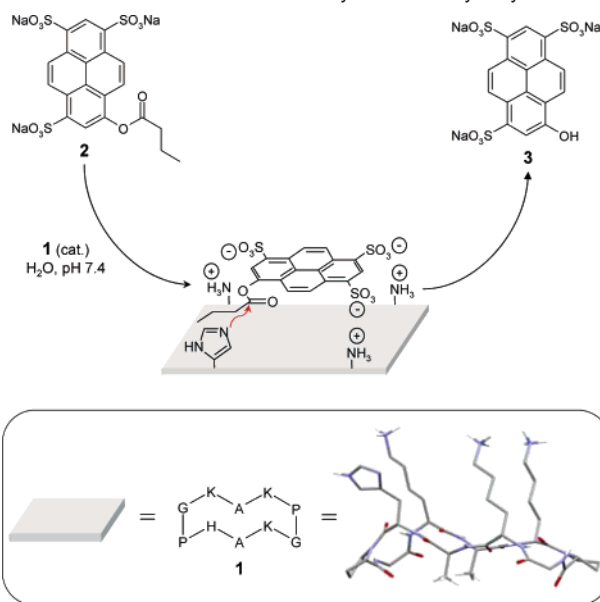
The development of specific sensors for (poly)anions is of considerable current interest since they play a fundamental role in a wide range of biological processes.¹ We decided to use enzyme-based sensors to achieve such a goal.² If the substrate or the product of an enzymatic reaction has distinguishable physical properties, specific inhibition of the catalytic activity by an anion of choice allows its detection. An interesting variation lies in the use of enzyme mimic-based sensors since they are a priori less fragile, more easily available, cheaper, and chemically more flexible (e.g., for subsequent immobilization) in comparison with their natural analogues. The activity and selectivity of native enzymes rely on complex folds for a precise spatial arrangement of a small number of catalytically important amino acids. Thus, the presentation of these functional groups on small peptides with well-defined secondary structures is an attractive alternative for the preparation of effective enzyme mimics.³

We designed the cyclic miniature esterase **1** that displays, in a controlled geometry⁴ and on a hypothetical rectangle of $\sim 5 \text{ \AA} \times \sim 7 \text{ \AA}$, three distinct positive charges (via the presence of lysines) for molecular recognition and a nucleophilic/basic center (via the presence of a histidine residue) for catalytic hydrolysis of the planar compound **2**, which displays itself three anionic charges and an ester function on a hypothetical rectangle of similar size (Scheme 1).⁵ We reasoned that this good topology match occurring between opposite charges of both partners should lead to the close proximity of the nucleophilic/basic nitrogen and the ester function and, as a result, should be responsible for ester hydrolysis rate enhancement. In addition, the hydrolysis product **3** (cascade blue) is an excellent fluorophore, furnishing therefore an optical signal that could potentially be modulated in presence of anionic species acting as inhibitors.⁶

Synthesis of peptide **1** was carried out by Fmoc strategy on chlorotrityl resin (500 mg, loading: 0.42 mmol/g), affording the protected linear peptide H-K(boc)-A-H(tr)-P-G-K(boc)-A-K(boc)-P-G-OH. Cyclization under high dilution conditions (0.5 mM) and subsequent deprotection gave the final product in good quantity (143 mg, overall yield 66%).⁷

Hydrolysis of **2** in water (Tris buffer, pH 7.4) was followed by fluorescence in a 96-well microliter-plate setup ($\lambda_{\text{exc}} = 460 \text{ nm}$, $\lambda_{\text{em}} = 530 \text{ nm}$). Enzyme-like kinetics was observed in the presence of **1** with multiple turnover activity (Figure 1A). A Michaelis–Menten model was applied to determine substrate binding $K_M = 135 \text{ \mu M}$, pseudo-first-order rate constant $k_{\text{cat}} = 0.0498 \text{ min}^{-1}$, rate enhancement $k_{\text{cat}}/k_{\text{uncat}} = 520$, and transition state dissociation constant $K_{\text{TS}} = K_M/(k_{\text{cat}}/k_{\text{uncat}}) = 0.260 \text{ \mu M}$ (Figure 1B). In the same conditions, catalysis by 4(5)-methylimidazole (MeIm) as reference catalyst was very inefficient (Figure 1A). A second-order $k_{\text{MeIm}} = 0.0124 \text{ mM}^{-1} \text{ min}^{-1}$ was measured at millimolar MeIm concentrations and used to calculate the catalytic enhancement $(k_{\text{cat}}/K_M)/k_{\text{MeIm}} = 30$. On the basis of a conservative mechanistic hypothesis

Scheme 1. Miniature Esterase-Catalyzed Ester Hydrolysis⁸



between MeIm and **1**, this rate enhancement was attributed to either nucleophilic or general base catalysis assisted by molecular recognition of the substrate; its modest magnitude probably also indicating that no cooperative effect occurs between amino acid residues.^{3c}

Then, we chose and tested a series of various metabolites carrying several negative charges (from two to six) as potential inhibitors of miniature esterase **1**. Whereas orthophosphate (Pi), AMP, *D*-myo-inositol-1,4,5-triphosphate (IP₃), citric acid, and ATP turned out to be null to moderate inhibitors (inhibition constants K_I up to 244 μM), ADP exhibited an unexpected parabolic Dixon plot (Figure 1C). This curvature is indicative of cooperative inhibition when more than one inhibitor molecule binds simultaneously to a catalyst.^{9,10} Hill plot analysis of the data (Figure 1D) was conducted and suggested a 2:1 complex between ADP and peptide **1** (Hill coefficient $n_H = 2.04$ and global dissociation constant $K_D = 52 \text{ \mu M}$).¹¹ A preliminary modeling study did not give us insight into the structure of such a ternary complex, which is probably the result of the subtle interplay of noncovalent interactions (e.g., stacking interactions between the nucleobases).

This large difference in affinity between **1** and the different anionic inhibitors, associated with the colorful property of **3**, permitted a convenient “naked-eye” detection of ADP directly from kinetic assays. In conditions where inhibitors are in enough excess relatively to **1** and **2** ($\geq 800 \text{ \mu M}$ for 200 μM of substrate **2** and 5 μM of peptide **1**), Pi, AMP, IP₃, ATP, or citric acid all lead to yellow-colored wells as a result of the formation of **3**, while the

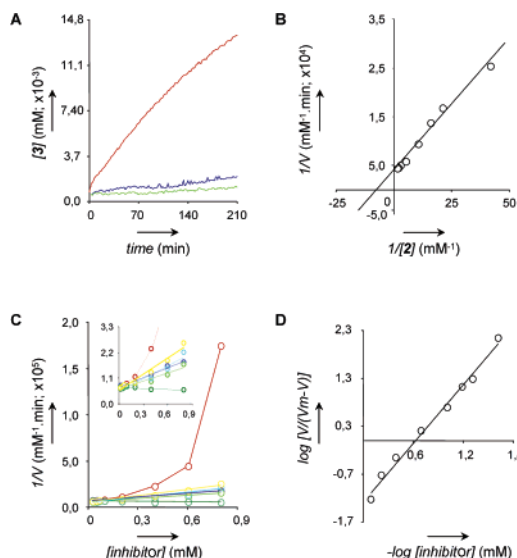


Figure 1. (A) Time plot formation of **3** from the hydrolysis of ester **2** (200 μ M) in the presence of catalytic peptide **1** (red) or 4-methylimidazole (blue), and background reaction (green). (B) Lineweaver–Burk plot of the hydrolysis of ester **2** with catalytic peptide **1**. (C) Dixon plots of the activity inhibition of peptide **1** by Pi (dark green), citric acid (light green), IP₃ (dark blue), AMP (light blue), ATP (yellow), and ADP (red). (D) Hill plot of the activity inhibition of catalytic peptide **1** by ADP. General conditions: 5 μ M catalyst **1** or 4(5)-methylimidazole, 24 °C, 20 mM Tris buffer pH 7.4.

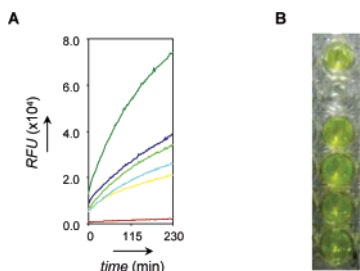


Figure 2. (A) Fluorescence versus time plot ($\lambda_{\text{exc}} = 460$ nm, $\lambda_{\text{em}} = 530$ nm) showing the formation of **3** from the hydrolysis of ester **2** in the presence of catalytic peptide **1** and ADP (red), ATP (yellow), AMP (light blue), citric acid (light green), IP₃ (dark blue), or Pi (dark green). RFU = relative fluorescence unit.¹² (B) Kinetic assay wells. From top to bottom: ATP, ADP, AMP, Pi, IP₃, and citric acid. General conditions: 800 μ M inhibitor, 5 μ M peptide **1**, and 200 μ M ester **2** in 20 mM Tris buffer pH 7.4, 24 °C.

ADP containing solution remains completely uncolored, even after 24 h reaction (Figure 2A,B).

This study shows that a cationic esterase mimic (**1**), which is responsible for the catalytic hydrolysis of a negatively charged fluorogenic ester (**2**), displays different inhibition behaviors in the presence of similar anionic metabolites in water and at physiological pH. On the contrary of the other negatively charged inhibitors tested, ADP strongly slowed down the formation of the fluorescent product (**3**) by virtue of cooperative inhibition, hence allowing its spectroscopic or visual detection. This result is remarkable since such ADP sensors, with good selectivity against ATP in particular, are poorly represented in the literature.¹³ Our sensor or its derivatives may

find future use in biological applications, such as protein kinase activity detection.¹⁴

Acknowledgment. This work was supported by the Centre National de la Recherche Scientifique, the Université Joseph Fourier de Grenoble, and the Institut Universitaire de France.

Supporting Information Available: Detailed synthetic and kinetic assays procedures, ES-MS spectrum of compound **1** (PDF). This material is available free of charge via the Internet at <http://pubs.acs.org>.

References

- (1) (a) Wiskur, S. L.; Ait-Haddou, H.; Lavigne, J. J.; Anslyn, E. V. *Acc. Chem. Res.* **2001**, *34*, 963–972. (b) Sessler, J. L.; Davis, J. M. *Acc. Chem. Res.* **2001**, *34*, 989–997. (c) Beer, P. D.; Gale, P. A. *Angew. Chem., Int. Ed.* **2001**, *40*, 486–516. (d) Anslyn, E. V. *J. Org. Chem.* **2007**, *72*, 687–699.
- (2) Moreno-Bondi, M.; Benito-Peña, E. In *Optical Chemical Sensors*; Baldini, F.; Chester, A. N.; Homola, J.; Martellucci, S., Eds.; Springer: The Netherlands, 2006; Vol. 224, pp 323–352.
- (3) For examples of peptide-based esterase mimics, see: (a) Esposito, A.; Delort, E.; Lagnoux, D.; Djojo, F.; Reymond, J.-L. *Angew. Chem., Int. Ed.* **2003**, *42*, 1381–1383. (b) Lagnoux, D.; Delort, E.; Douat-Casassus, C.; Esposito, A.; Reymond, J.-L. *Chem.—Eur. J.* **2004**, *10*, 1215–1226. (c) Douat-Casassus, C.; Darbre, T.; Reymond, J.-L. *J. Am. Chem. Soc.* **2004**, *126*, 7817–7826. (d) Clouet, A.; Darbre, T.; Reymond, J.-L. *Adv. Synth. Catal.* **2004**, *346*, 1195–1204. (e) Delort, E.; Darbre, T.; Reymond, J.-L. *J. Am. Chem. Soc.* **2004**, *126*, 15642–15643. (f) Delort, E.; Nguyen-Trung, N.-Q.; Darbre, T.; Reymond, J.-L. *J. Org. Chem.* **2006**, *71*, 4468–4480. (g) Broo, K. S.; Brive, L.; Ahlberg, P.; Baltzer, L. *J. Am. Chem. Soc.* **1997**, *119*, 11362–11372. (h) Kerstin, S.; Nilsson, H.; Nilsson, J.; Baltzer, L. *J. Am. Chem. Soc.* **1998**, *120*, 10287–10295. (i) Baltzer, L. K.; Broo, S.; Nilsson, H.; Nilsson, J. *Bioorg. Med. Chem.* **1999**, *7*, 83–91. (j) Nilsson, J.; Baltzer, L. *Chem.—Eur. J.* **2000**, *6*, 2214–2220. (k) Andersson, L. K.; Caspersson, M.; Baltzer, L. *Chem.—Eur. J.* **2002**, *8*, 3687–3689. (l) Bolon, D. L.; Mayo, S. L. *Proc. Natl. Acad. Sci. U.S.A.* **2001**, *98*, 14274–14279. (m) Wei, Y.; Hecht, M. H. *Protein Eng. Des.* **2004**, *17*, 67–75. (n) Nicoll, A. J.; Allemann, R. K. *Org. Biomol. Chem.* **2004**, *2*, 2175–2180. (o) Baumeister, B.; Sakai, N.; Matile, S. *Org. Lett.* **2001**, *3*, 4229–4232. (p) Som, A.; Sakai, N.; Matile, S. *Bioorg. Med. Chem.* **2003**, *11*, 1363–1369.
- (4) The presence of two prolylglycine sequences as β type II turn inducers constrains the peptide conformation into an antiparallel β -sheet. For a review on this family of decapeptidic scaffold, see: Singh, Y.; Dolphin, G.; Razkin, J.; Dumy P. *ChemBioChem* **2006**, *7*, 1298–1314.
- (5) A similar design approach has been employed by Matile and co-workers. See refs 3o and 3p.
- (6) Wolfbeis, O. S.; Koller, E. *Anal. Biochem.* **1983**, *129*, 365–370.
- (7) Garanger, E.; Boturny, D.; Renaudet, O.; Defrancq, E.; Dumy, P. *J. Org. Chem.* **2006**, *71*, 2402–2410.
- (8) The three-dimensional model was built without energy minimization from a previously reported X-ray structure of a similar cyclic peptide. The original *p*-nitrobenzyl residues were simply replaced with lysine and histidine side chains. Some hydrogen atoms have been omitted for clarity. Peluso, S.; Ruckle, T.; Lehmann, C.; Mutter, M.; Peggion, C.; Crisma, M. *ChemBioChem* **2001**, *2*, 432–437.
- (9) Segel, I. H. *Enzyme Kinetics: Behavior and Analysis of Rapid Equilibrium and Steady-State Enzyme Systems*; Wiley: New York, 1993; pp 465–504.
- (10) Peptide **1** did not catalyze the hydrolysis of ADP in the conditions used in this study.
- (11) Parameters were calculated using the Hill equation: $\log [V/(V_m - V)] = -n_H \log [\text{inhibitor}] + \log K_D$, where n_H , V_m , and K_D are the Hill coefficient, the maximum velocity, and the global dissociation constant, respectively.
- (12) The curve shift on the y-axis at $t = 0$ is related to the time delay that occurred between the sample preparation and the beginning of the spectroscopic measurement.
- (13) For nice examples, see: (a) Aguilar, J. A.; Garcia-Espana, E.; Guerrero, J. A.; Luis, S. V.; Llinares, J. M.; Miravet, J. F.; Ramirez, J. A.; Soriano, C. *Chem. Commun.* **1995**, 2237–2239. (b) Brune, M.; Corrie, J. E. T.; Webb, M. R. *Biochemistry* **2001**, *40*, 5087–5094. (c) Butterfield, S. M.; Waters, M. L. *J. Am. Chem. Soc.* **2003**, *125*, 9580–9581. (d) Srinivasan, J.; Cload, S. T.; Hamaguchi, N.; Kurz, J.; Keene, S.; Kurz, M.; Boomer, R. M.; Blanchard, J.; Epstein, D.; Wilson, C.; Diener, J. L. *Chem. Biol.* **2004**, *11*, 499–508. (e) Litvinchuk, S.; Sordé, N.; Matile, S. *J. Am. Chem. Soc.* **2005**, *127*, 9316–9317.
- (14) (a) Das, G.; Talukdar, P.; Matile, S. *Science* **2002**, *298*, 1600–1602. (b) Goddard, J.-P.; Reymond, J.-L. *Trends Biotechnol.* **2004**, *22*, 363–370.

JA070734C